DE-Vol. 70, Mechanism Synthesis and Analysis
ASME 1994

DESIGN OF THE SPATIAL 4C MECHANISM FOR RIGID BODY GUIDANCE

Pierre Larochelle and J. Michael McCarthy
Department of Mechanical and Aerospace Engineering
University of California, Irvine
Irvine, California

Abstract

In this paper we present an algebraic formulation for the constraint manifold of the spatial CC dyad in the image space of spatial displacements. We then present a technique, utilizing the constraint manifold, for performing the dimensional synthesis of mechanisms for rigid body guidance through n positions. Finally, we present numerical results for 10 prescribed positions for the coupler of a spatial $4C$ mechanism.

1 Introduction

In Bodduluri 1991 the solution to four position rigid body guidance for the spatial $4C$ mechanism was presented. Here we extend the works of Ravani and Roth 1983, Bodduluri 1990, and McCarthy 1991 to the dimensional synthesis of spatial $4C$ mechanisms for n position rigid body guidance, see Fig. 1. The first step of the design process is to define the design goal of the mechanism in terms of the desired positions of the moving body. In the case of $4C$ mechanisms, if more than 5 positions are specified there will be, in general, no exact solution, see Suh and Radcliffe 1978. That is to say, there will be no mechanism which passes precisely through all of the desired positions. Therefore, we utilize an optimization procedure first derived by Ravani and Roth 1983 by which we vary the synthesis variables so as to minimize the position error of the mechanism.

The optimization algorithm involves writing the kinematic constraint equation of the CC dyad using the components of a dual quaternion. We view these equations as constraint manifolds in the image space of spatial displacements, see Bottema and Roth 1979 and McCarthy 1990. The result is an analytical representation of the workspace of the dyad which is parameterized by its dimensional synthesis variables. We then combine two CC dyads to form a $4C$ closed chain. The constraint manifold of the $4C$ mechanism is simply the intersection of the constraint manifolds of its two CC sub chains. This intersection provides an analytical representation of the workspace of the $4C$ mechanism in the image space of spatial displacements. The optimization goal is to vary the design variables such that all of the prescribed positions are either: (1) in the workspace, or, (2) the workspace comes as close as possible to all of the desired positions. In what follows, we apply the optimization algorithm to the design of spatial four bar mechanisms with four cylindric joints, the $4C$ mechanism, and illustrate the procedure by an example for 10 desired positions.

2 Spatial Displacements

First, we review the use of dual quaternions for describing spatial displacements.

A general spatial displacement may be described by a 3×3 orthonormal rotation matrix $[A]$ and a displacements vector $\mathbf{d} = (d_x, d_y, d_z)^T$. Associated with the matrix of rotation $[A]$ is an axis of rotation

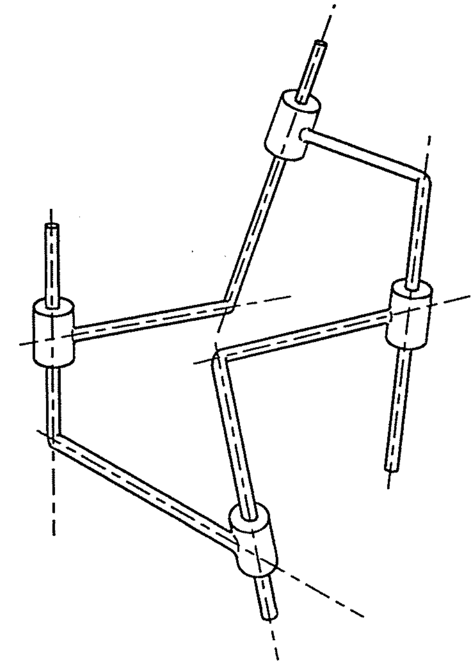

Figure 1: A Spatial $4C$ Mechanism

s and a rotation angle about that axis θ.

Using the translation vector $\mathbf{d}$, the rotation axis s, and the rotation angle θ, we can represent the spatial displacement by the eight dimensional vector, $\tilde{\mathbf{q}}$, which is written as, see McCarthy, 1990,

$$
\begin{aligned}
q_1 &= s_x \sin\frac{\theta}{2} \\
q_2 &= s_y \sin\frac{\theta}{2} \\
q_3 &= s_z \sin\frac{\theta}{2} \\
q_4 &= \cos\frac{\theta}{2} \\
q_5 &= \frac{(-d_z q_2 + d_y q_3 + d_x q_4)}{2} \\
q_6 &= \frac{(d_z q_1 - d_x q_3 + d_y q_4)}{2} \\
q_7 &= \frac{(-d_y q_1 + d_x q_2 + d_z q_4)}{2} \\
q_8 &= \frac{(-d_x q_1 - d_y q_2 - d_z q_3)}{2}
\end{aligned}
\tag{1}
$$

We refer to $\tilde{\mathbf{q}}$ as a dual quaternion. The components of $\tilde{\mathbf{q}}$ satisfy,

$$
\begin{aligned}
G_1(\tilde{\mathbf{q}}) &: q_1^2 + q_2^2 + q_3^2 + q_4^2 - 1 = 0 \\
G_2(\tilde{\mathbf{q}}) &: q_1 q_5 + q_2 q_6 + q_3 q_7 + q_4 q_8 = 0
\end{aligned}
\tag{2}
$$

Note that $\tilde{\mathbf{q}}$, given by Eq. 1, is an eight dimensional vector which satisfies the two constraint equations, Eqs. 2, therefore, the components of $\tilde{\mathbf{q}}$ form a six dimensional algebraic manifold. We denote this manifold as *the image space of spatial displacements.*

The rotation matrix, $[A]$, and the translation vector, $\mathbf{d}$, can be recovered from the dual quaternion, $\tilde{\mathbf{q}}$, describing a spatial displacement as follows,

$$
[A] = \tag{3}
$$

$$
\begin{bmatrix}
q_1^2 - q_2^2 - q_3^2 + q_4^2 & 2(q_1q_2 - q_3q_4) & 2(q_1q_3 + q_2q_4) \\
2(q_1q_2 + q_3q_4) & -q_1^2 + q_2^2 - q_3^2 + q_4^2 & 2(q_2q_3 - q_1q_4) \\
2(q_1q_3 - q_2q_4) & 2(q_2q_3 + q_1q_4) & -q_1^2 - q_2^2 + q_3^2 + q_4^2
\end{bmatrix}
$$

$$
\mathbf{d} = 2 \begin{bmatrix} -q_8 & q_7 & -q_6 & q_5 \\ -q_7 & -q_8 & q_5 & q_6 \\ q_6 & -q_5 & -q_8 & q_7 \end{bmatrix} \begin{pmatrix} q_1 \\ q_2 \\ q_3 \\ q_4 \end{pmatrix} \tag{4}
$$

Equations 3 and 4 will be central to our derivation of the constraint manifold of the CC dyad.

3 Constraint Manifolds

In this section we derive the algebraic constraint manifold of the spatial CC dyad. This dyad may be combined serially to form a complex open chain or, when connected back to the fixed link, may be joined so as to form a closed chain; a mechanism or linkage.

The continuous motion of the end link of an open chain maps into a constraint manifold in the image space. For closed chains the constraint manifold of the mechanism is the intersection of the constraint manifolds of its open subchains.

The constraint manifolds are derived by using the geometric conditions that the joints of the dyad impose on the moving body. The vector equations for the geometric constraints are based upon the work of Suh and Radcliffe, 1978, and Bodduluri, 1990. Using the rotation matrix and translation vector, expressed by the image space coordinates and the geometric constraint equations of the dyad we arrive at algebraic constraint equations in the image space that are parameterized by the dimensional synthesis variables of the dyad.

3.1 Spatial *CC* Dyad

A *CC* dyad is shown in Fig. 2. Let the axis of the fixed joint be specified by the dual vector, $\hat{\mathbf{u}} = \mathbf{u} + \epsilon\mathbf{u}^0$, measured in the fixed reference frame and let the moving axis be specified by, $\hat{\boldsymbol{\lambda}} = \boldsymbol{\lambda} + \epsilon\boldsymbol{\lambda}^0$, measured in the moving frame, M. Let us define the dual vector $\hat{\mathbf{l}}$ as representing the moving axis $\hat{\boldsymbol{\lambda}}$ as measured in the fixed frame F. The dual vectors $\hat{\mathbf{l}}$ and $\hat{\boldsymbol{\lambda}}$ are related by the dual orthogonal matrix $[\hat{A}]$, where $[\hat{A}] = [A] + \epsilon[D][A]$, and $[D]$ is the 3×3 skew-symmetric matrix from the translation vector $\mathbf{d}$.

$$\hat{\mathbf{l}} = [\hat{A}]\hat{\boldsymbol{\lambda}} \tag{5}$$

Eq. 5 can be expanded and rewritten as,

$$\hat{\mathbf{l}} = \mathbf{l} + \epsilon\mathbf{l}^0 = [A]\boldsymbol{\lambda} + \epsilon([A]\boldsymbol{\lambda}^0 + [D][A]\boldsymbol{\lambda}) \tag{6}$$

Because the two axes are connected by a rigid link we have that $\hat{\alpha} = (\alpha, a)$ must remain constant.

$$\hat{\mathbf{u}} \cdot \hat{\mathbf{l}} = \hat{\mathbf{u}} \cdot [\hat{A}]\hat{\boldsymbol{\lambda}} = \cos\hat{\alpha} \tag{7}$$

We substitute Eq. 6 into Eq. 7 and obtain,

$$\mathbf{u} \cdot [A]\boldsymbol{\lambda} + \epsilon\left\{\mathbf{u} \cdot ([A]\boldsymbol{\lambda}^0 + [D][A]\boldsymbol{\lambda}) + \mathbf{u}^0 \cdot [A]\boldsymbol{\lambda}\right\} = \cos\alpha - \epsilon a \sin\alpha \tag{8}$$

From the real part of Eq. 8 we obtain the constant twist condition,

$$\mathbf{u} \cdot [A]\boldsymbol{\lambda} - \cos\alpha = 0 \tag{9}$$

From the dual part of Eq. 8 we obtain the constant moment condition as,

$$\mathbf{u} \cdot ([A]\boldsymbol{\lambda}^0 + [D][A]\boldsymbol{\lambda}) + \mathbf{u}^0 \cdot [A]\boldsymbol{\lambda} + a\sin\alpha = 0 \tag{10}$$

Equations 9 and 10 are the implicit constraint equations for a spatial *CC* dyad.

To obtain an algebraic expression for the constraint manifold in the image space of spatial displacements we substitute Equations 3 and 4 into the constraint equations, Eq. 9 and Eq. 10, to yield,

$CC_1(\tilde{\mathbf{q}}, \mathbf{r})$:

$$\mathbf{u} \cdot [A(\tilde{\mathbf{q}})]\boldsymbol{\lambda} - \cos\alpha = 0 \tag{11}$$

$CC_2(\tilde{\mathbf{q}}, \mathbf{r})$:

$$\mathbf{u} \cdot ([A(\tilde{\mathbf{q}})]\boldsymbol{\lambda}^0 + [D(\tilde{\mathbf{q}})][A(\tilde{\mathbf{q}})]\boldsymbol{\lambda}) + \mathbf{u}^0 \cdot [A(\tilde{\mathbf{q}})]\boldsymbol{\lambda} + a\sin\alpha = 0 \tag{12}$$

The 14 dimensional design vector $\mathbf{r}$ for a spatial *CC* dyad is therefore,

$$\mathbf{r} = \begin{pmatrix} \mathbf{u} \\ \mathbf{u}^0 \\ \boldsymbol{\lambda} \\ \boldsymbol{\lambda}^0 \\ \alpha \\ a \end{pmatrix} \tag{13}$$

where $\hat{\mathbf{u}}$ and $\hat{\boldsymbol{\lambda}}$ specify the fixed and moving C joints of the dyad and finally α is the twist and a is the normal length of the *CC* link.

4 Fitting Image Curves

We now describe the method described by Ravani and Roth, 1983, to perform dimensional synthesis using constraint manifolds. The first step is to formulate the constraint manifold of the mechanism. In the case of a closed chain, such as a spatial 4*C* mechanism, this involves two spatial *CC* dyads. The equations of the constraint manifolds of the dyads and the dual quaternion constraint equation are combined to form the complete constraint manifold $CM(\tilde{\mathbf{q}}, \mathbf{r})$.

$$CM(\tilde{\mathbf{q}}, \mathbf{r}) : \begin{pmatrix} CC_a(\tilde{\mathbf{q}}, \mathbf{r}) \\ CC_b(\tilde{\mathbf{q}}, \mathbf{r}) \\ G_1(\tilde{\mathbf{q}}) \\ G_2(\tilde{\mathbf{q}}) \end{pmatrix} = \mathbf{0} \tag{14}$$

where $CC_a(\tilde{\mathbf{q}}, \mathbf{r})$ and $CC_b(\tilde{\mathbf{q}}, \mathbf{r})$ are from Equations 11 and 12 written for each dyad of the mechanism, $G_1(\tilde{\mathbf{q}})$ and $G_2(\tilde{\mathbf{q}})$ are the dual quaternion constraint equations, Eq. 2, and $\mathbf{r}$ is the vector of dimensional synthesis variables.

Here, the goal is to determine the design variables, $\mathbf{r}$, so that the constraint manifold passes through, or

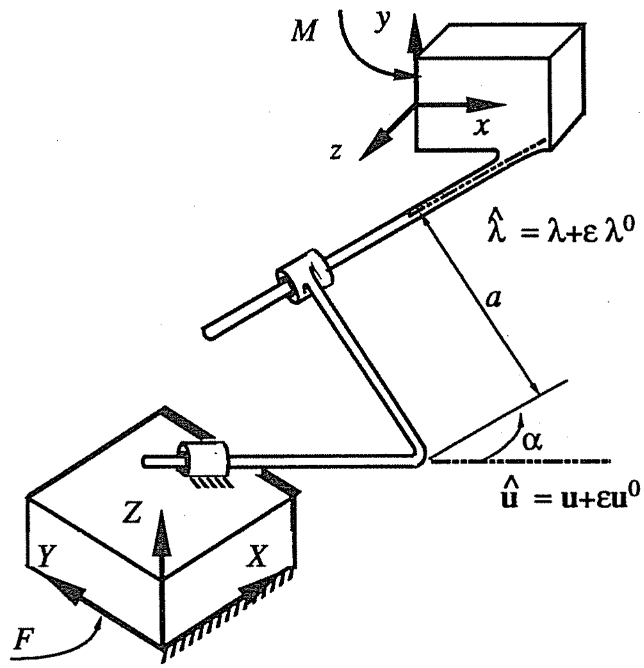

Figure 2: A Spatial CC Dyad

as close as possible to, n desired points in the image space. Let $\tilde{\mathbf{q}}_d$ represent one desired point in the image space; either a dual quaternion, quaternion, or planar quaternion. We assume that $\tilde{\mathbf{q}}_d$ does not lie on the constraint manifold and write a Taylor series expansion of the constraint manifold about $\tilde{\mathbf{q}}_d$. In other words, we approximate the level surface of the image curve through $\tilde{\mathbf{q}}_d$ by its tangent hyperplane.

$$CM(\tilde{\mathbf{q}}_d, \mathbf{r}) + \frac{\partial CM(\tilde{\mathbf{q}}_d, \mathbf{r})}{\partial \tilde{\mathbf{q}}_d}(\tilde{\mathbf{q}} - \tilde{\mathbf{q}}_d) = 0 \qquad (15)$$

Let us now reformulate Eq. 15 as a system of linear equations,

$$[J]\mathbf{x} = \mathbf{b} \qquad (16)$$

where, $[J]$ is the matrix of partial derivatives of $CM(\tilde{\mathbf{q}}, \mathbf{r})$, $\mathbf{b} = -CM(\tilde{\mathbf{q}}_d, \mathbf{r})$, and $\mathbf{x} = \tilde{\mathbf{q}} - \tilde{\mathbf{q}}_d$. In general there will be infinite solutions to Eq. 16. Therefore, we seek the minimum norm solution of Eq. 16. Note that $\mathbf{x}$ is in some sense a measure of the "distance" from $\tilde{\mathbf{q}}_d$ to $CM(\tilde{\mathbf{q}}, \mathbf{r})$ and that even though this metric is usefull for designing mechanisms it possesses the undesirable characteristic of being variant with respect to choice of coordinate system when used for designing planar and spatial mechanisms. Unfortunately the metric's dependency upon choice of coordinate system is to be expected for as has been stated by several researchers in the field there is no bi-invariant metric for planar and spatial motions, see Kazerounian and Rastegar 1992, and Duffy 1990.

The minimum norm solution of Eq. 16 is found by minimizing the Lagrangian function,

$$\Lambda(\mathbf{x}, \mathbf{b}) = \mathbf{x}^T\mathbf{x} + \boldsymbol{\lambda}^T([J]\mathbf{x} - \mathbf{b}) \qquad (17)$$

where $\boldsymbol{\lambda}$ is a vector of Lagrange multipliers. The minimum of Eq. 17 is found when,

$$\frac{\partial \Lambda}{\partial \mathbf{x}} = 2\mathbf{x}^* + \boldsymbol{\lambda}^T[J] = 0 \qquad (18)$$

We now combine Eq. 16 with Eq. 18 to form the following system of equations,

$$\begin{bmatrix} [J] & [0] \\ 2[I] & [J]^T \end{bmatrix} \begin{pmatrix} \mathbf{x}^* \\ \boldsymbol{\lambda} \end{pmatrix} = \begin{pmatrix} \mathbf{b} \\ 0 \end{pmatrix} \qquad (19)$$

We solve Eq. 19, by use of the pseudo inverse of $[J]$, to yield,

$$\mathbf{x}^* = [J]^T([J][J]^T)^{-1}\mathbf{b} \qquad (20)$$

From the definition of $\mathbf{x}$ we have,

$$\tilde{\mathbf{q}}^* = \tilde{\mathbf{q}}_d + \mathbf{x}^* \qquad (21)$$

where $\tilde{\mathbf{q}}^*$ approximates the point on the constraint manifold closest to $\tilde{\mathbf{q}}_d$. Moreover, we may use $\tilde{\mathbf{q}}^*$ to

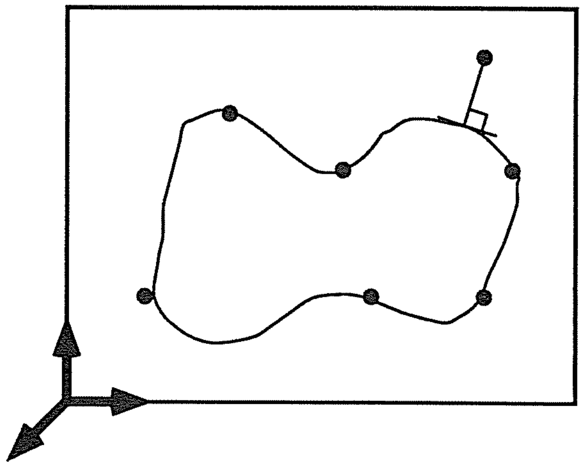

Figure 3: A Representation of Normal Image Curve Fitting

approximate the normal distance, $e(\mathbf{r})$, from $\tilde{\mathbf{q}}_d$ to the constraint manifold,

$$e(\mathbf{r})^2 = (\tilde{\mathbf{q}}^* - \tilde{\mathbf{q}}_d)^T(\tilde{\mathbf{q}}^* - \tilde{\mathbf{q}}_d) = \|[J]^T([J][J]^T)^{-1}\mathbf{b}\|^2 \quad (22)$$

Finally, performing n position synthesis requires computing $e(\mathbf{r})$ for each desired position, $\tilde{\mathbf{q}}_d$. The total error, $E(\mathbf{r})$, is then given by,

$$E(\mathbf{r}) = \sum_{i=1}^{n} e_i^2(\mathbf{r}) \quad (23)$$

Thus, we have formulated the n position dimensional synthesis problem into the form of a minimization problem with objective function $E(\mathbf{r})$. In abstraction, we are manipulating the dimensional synthesis variables, $\mathbf{r}$, such that the image curve of the mechanism passes through, or comes as close as possible to, the set of desired positions, $\tilde{\mathbf{q}}_d$. A planar representation of this methodology of image curve fitting is illustrated in Fig. 3. Here, the desired positions are the points in the image space and the simple closed curve is the constraint manifold. We estimate the normal distance from the curve to the points using a tangent approximation to the curve and seek to minimize this distance for all desired points.

5 The Optimization Problem

Having derived the objective function, we are now able to formally pose our design objective for n positions in the form of an unconstrained optimization problem.

Pos.	X	Y	Z	Long.	Lat.	Roll
1	1.0	0.0	5.0	100.0	0.0	0.0
2	2.0	0.0	4.0	90.0	0.0	10.0
3	3.0	0.0	3.0	80.0	0.0	20.0
4	4.0	0.0	2.0	70.0	0.0	30.0
5	5.0	0.0	1.0	60.0	0.0	40.0
6	6.0	0.0	−1.0	50.0	0.0	50.0
7	7.0	0.0	−2.0	40.0	0.0	60.0
8	8.0	0.0	−3.0	30.0	0.0	70.0
9	9.0	0.0	−4.0	20.0	0.0	80.0
10	10.0	0.0	−5.0	10.0	0.0	90.0

Table 1: The 10 Desired Positions

$$\begin{array}{ll} \text{Minimize:} & E(\mathbf{r}) \\ \text{Given:} & \tilde{\mathbf{q}}_1, \tilde{\mathbf{q}}_2, \tilde{\mathbf{q}}_3, \ldots, \tilde{\mathbf{q}}_n \end{array} \quad (24)$$

where $E(\mathbf{r})$ is given by Eq. 23, $\tilde{\mathbf{q}}_1, \tilde{\mathbf{q}}_2, \tilde{\mathbf{q}}_3, \ldots, \tilde{\mathbf{q}}_n$ are the desired positions, and $\mathbf{r}$ is the design vector of the mechanism, containing the design vectors of each of the mechanism's dyads.

6 Case Study

In this section we present an example of the design of a spatial $4C$ mechanism for 10 position rigid body guidance. The 10 desired positions are listed in Tbl. 1 and shown in perspective projection in Figs. 5, 6, and 7 where the solid is the moving body drawn coincident with the fixed reference frame and the 10 desired positions of the moving body are drawn in wireframe. The 28 dimensional design vector $\mathbf{r}$ is defined in Tbl. 3, where $\hat{\mathbf{u}}$ and $\hat{\boldsymbol{\lambda}}$ are the fixed and moving axes of each dyad,(a, b), and $\hat{\alpha}$ is the corresponding crank length. In general, Eq. 24 is difficult to solve. We have found the Levenberg-Marquardt algorithm to be a powerful tool in obtaining solutions to Eq. 24. Specifically, we have used the version of the algorithm found in the **ZXSSQ** subroutine of the IMSL *FORTRAN* library. The results of the design procedure are listed in Tbl. 2 and Tbl. 3. In Fig. 4 we illustrate graphically the rigid body in its approximation to position 4. The actual position of the moving body is drawn as the solid and the desired position of the moving body is shown in wireframe.

Pos.	Initial Error	Final Error
1	6.02E+0	1.00E−1
2	4.10E+0	5.87E−3
3	3.46E+0	1.05E−2
4	4.64E+0	2.86E−3
5	8.77E+0	3.27E−2
6	1.77E+1	5.80E−2
7	3.02E+1	3.97E−2
8	4.83E+1	3.77E−2
9	1.33E+2	2.02E−2
10	1.71E+3	4.78E−2
	$\sum = 1.97E{+}3$	$\sum = 3.56E{-}1$

Table 2: Spatial $4C$ Synthesis: Position Results

Design Vector $\mathbf{r}$		
Definition	Initial Guess	Final Design
$\mathbf{u}_a$	0.25900	0.17766
	0.54510	−0.90343
	0.79730	0.39020
$\mathbf{u}_a^0$	−0.56810	8.37209
	1.29390	−1.64961
	−0.70010	−7.63127
$\boldsymbol{\lambda}_a$	0.70710	0.68875
	0.00000	0.00853
	0.70710	0.72495
$\boldsymbol{\lambda}_a^0$	0.00000	0.00014
	−0.70710	−0.72524
	0.00000	0.00840
α_a	1.38110	1.84000
a_a	0.05970	−8.06718
$\mathbf{u}_b$	0.23240	0.23824
	0.62980	−0.85396
	0.74120	0.46260
$\mathbf{u}_b^0$	−0.52190	9.04575
	0.71340	−1.62358
	−0.44250	−7.65567
$\boldsymbol{\lambda}_b$	0.89440	0.88249
	0.00000	−0.01195
	0.44720	0.47018
$\boldsymbol{\lambda}_b^0$	0.44720	0.47000
	−0.44720	−0.47005
	−0.89440	−0.89410
α_b	1.61160	2.05004
a_b	1.59260	−8.17927

Table 3: Spatial $4C$ Synthesis: Optimization Results

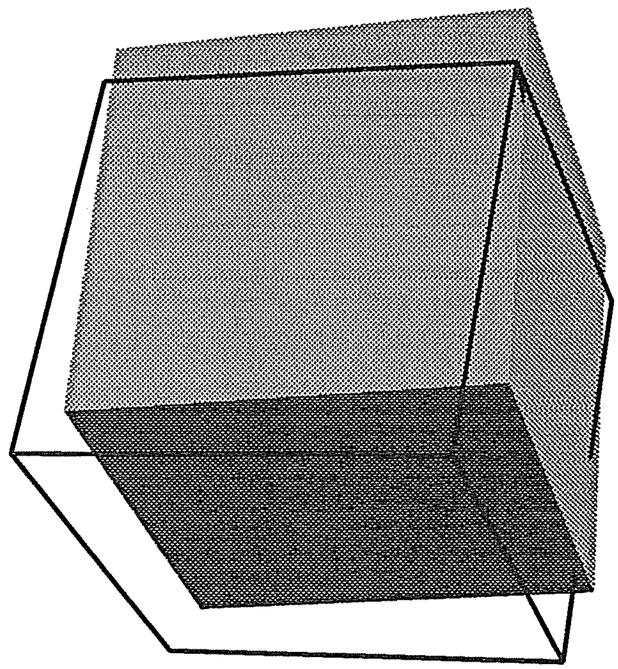

Figure 4: Results for Position 4

7 Conclusion

In this paper we have presented our development of an algorithm, originally proposed by Ravani and Roth 1983, for the dimensional synthesis of spatial $4C$ mechanisms for n position rigid body guidance. The synthesis procedure utilizes an algebraic formulation for the constraint manifold of the CC dyad to define the workspace of the $4C$ mechanism in the image space of spatial displacements. The result of the optimization is the set of design variables such that the workspace of the mechanism contains, or comes as close as possible to, the n desired positions.

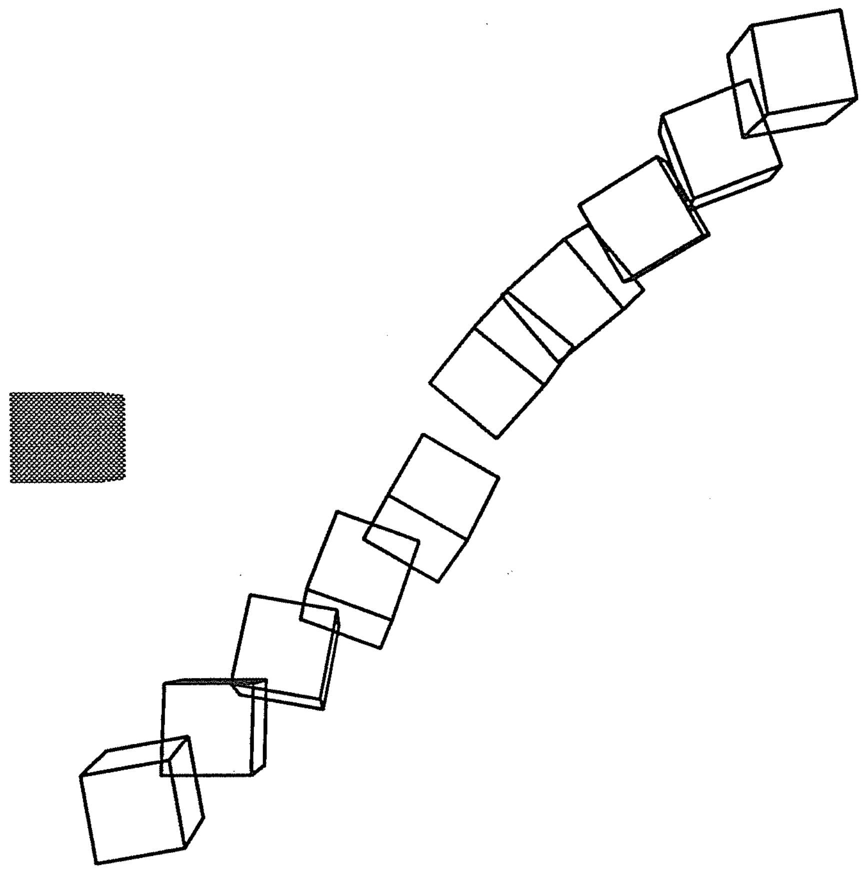

Figure 5: The 10 Positions: top view

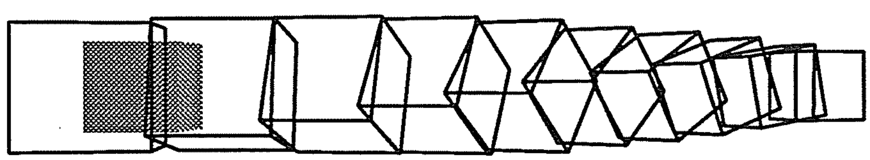

Figure 6: The 10 Positions: front view

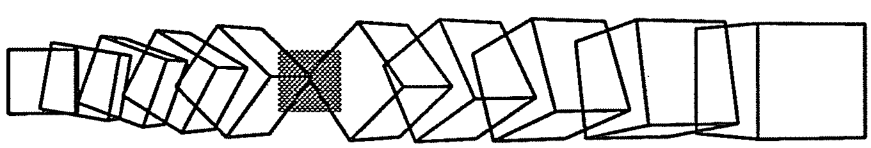

Figure 7: The 10 Positions: side view

References

[1] Bodduluri, R.M.C., Design and Planned Movement of Multi-Degree of Freedom Spatial Mechanisms. *Ph.D. Dissertation.* University of California, Irvine, 1990.

[2] Bodduluri, R.M.C., Interactive Graphics for Four Position Synthesis of $4C$ Spatial Mechanisms. 8^{th} *World Congress of the IFToMM.* August, 1991.

[3] Bottema, O. and Roth, B., *Theoretical Kinematics.* North-Holland, Amsterdam, 1979.

[4] Duffy, J., Editorial: The Fallacy of Modern Hybrid Control Theory that is Based Upon "Orthogonal Complements" of Twists and Wrench Spaces. *J. of Robotic Systems.* 7(2):139-144, 1990.

[5] Kazerounian, K., and Rastegar, J., Object Norms: A Class of Coordinate and Metric Independent Norms for Displacements. *Proc. of the 1992 ASME Design Technical Conferences.* DE-Vol 47:271-275, September 1992.

[6] McCarthy, J.M., *An Introduction to Theoretical Kinematics.* MIT Press, 1990.

[7] McCarthy, J.M., Finite Position Synthesis of a $4S$ Spatial Mechanism Using Kinematic Mapping Motion Synthesis Using Kinematic Mappings. 8^{th} *World Congress of the IFToMM.* August, 1991.

[8] Ravani, B., and Roth, B., Motion Synthesis Using Kinematic Mappings. *ASME Journal Mechanisms, Transmissions, and Automation in Design.* 105:460-467, September 1983.

[9] Suh, C.H., and Radcliffe, C.W., *Kinematics and Mechanism Design.* John Wiley and Sons, 1978.